agronomy

MDPI

Article

Design and Testing of a Pneumatic Jujube Harvester

Huaming Hou [1,2,†], Wei Niu [1,†], Qixian Wen [1], Hairui Yang [1], Jianming Zhang [1], Rui Zhang [1], Bing Xv [1,2] and Qingliang Cui [1,2,*]

[1] College of Agricultural Engineering, Shanxi Agricultural University, Taigu 030801, China; houhuaming@sxau.edu.cn (H.H.); 20232076@stu.sxau.edu.cn (W.N.); 202430058@stu.sxau.edu.cn (Q.W.); 202430062@stu.sxau.edu.cn (H.Y.); 202530207@stu.sxau.edu.cn (J.Z.); 202430068@stu.sxau.edu.cn (R.Z.); xub@sxau.edu.cn (B.X.)

[2] Dryland Farm Machinery Key Technology and Equipment Key Laboratory of Shanxi Province, Taigu 030801, China

* Correspondence: qlcui@sxau.edu.cn

† These authors contributed equally to this work and should be regarded as co-first authors.

Abstract

Jujubes have a beautiful taste, and high nutritional and economic value. The planting area of dwarf and densely planted jujubes is large and shows an increasing trend; however, the mechanization level and efficiency of fresh jujube harvesting are low. For this reason, our research group conducted a study on mechanical harvesting technology for fresh jujubes. A pneumatic jujube harvester was designed. This harvester is composed of a self-regulating picking mechanism, a telescopic conveying pipe, a negative pressure generator, a cleaning mechanism, a double-chamber collection box, a single-door shell, a control assembly, a generator, a towing mobile chassis, etc. During the harvest, the fresh jujubes on the branches are picked under the combined effect of the flexible squeezing of the picking roller and the suction force of the negative pressure air flow. They then enter the cleaning mechanism through the telescopic conveying pipe. Under the combined effect of the upper and lower baffles of the cleaning mechanism and the negative-pressure air flow, the fresh jujubes are separated from impurities such as jujube leaves and branches. The clean fresh jujubes fall into the collection box. We considered the damage rate of fresh jujubes, impurity rate, leakage rate, and harvesting efficiency as the indexes, and the negative-pressure suction wind speed, picking roller rotational speed, and the inclination angle of the upper and lower baffles of the cleaning and selection machinery as the test factors, and carried out the harvesting test of fresh jujubes. The test results show that when the negative-pressure suction wind speed was 25 m/s, the picking roller rotational speed was 31 r/min, and the inclination angles of the upper and lower baffle plates for cleaning and selecting were −19° and 19.5°, respectively, the breakage rate of fresh jujube harvesting was 0.90%, the rate of impurity was 1.54%, the rate of leakage was 2.59%, and the efficiency of harvesting was 73.37 kg/h, realizing the high-efficiency and low-loss harvesting of fresh jujubes. This study provides a reference for the research and development of fresh jujube mechanical harvesting technology and equipment.

Keywords: mechanical design; harvester; fresh jujube; pneumatic; harvesting trials

check for updates

Academic Editor: Marco Fontanelli

Received: 17 June 2025
Revised: 18 July 2025
Accepted: 30 July 2025
Published: 3 August 2025

Citation: Hou, H.; Niu, W.; Wen, Q.; Yang, H.; Zhang, J.; Zhang, R.; Xv, B.; Cui, Q. Design and Testing of a Pneumatic Jujube Harvester. *Agronomy* **2025**, *15*, 1881. https://doi.org/10.3390/agronomy15081881

Copyright: © 2025 by the authors. Licensee MDPI, Basel, Switzerland. This article is an open access article distributed under the terms and conditions of the Creative Commons Attribution (CC BY) license (https://creativecommons.org/licenses/by/4.0/).

1. Introduction

As an important economic fruit unique to China, jujubes have a long history of cultivation and a wide range of planting areas. China is the world's largest producer of jujubes, with the cultivated area and output of jujubes ranking first in the world. The date

industry plays an important role in promoting regional economic development, increasing farmers' income and improving the ecological environment [1].

In the global jujube industry, China occupies a pivotal position. However, China's jujube harvesting chain faces many challenges. At present, the domestic jujube harvesting mode is mainly manual, while mechanized harvesting accounts for a relatively small proportion. During the ripening period, about 70% of the dried jujubes fall off due to the natural breakage of the fruit stalk or wind force, while the remaining portion need to be manually knocked on the branches to make them fall off and then picked up one by one by hand to be crated. This type of operation is extremely labor-intensive, with poor working conditions and low harvesting efficiency [2].

International research has focused on generalized technologies and equipment for forest fruit harvesting. With the help of new materials, new agronomy, mechatronics, 3S, and other advanced technologies, the mechanization of foreign fruit harvesting is moving in an intelligent, efficient, comfortable direction and has realized a series of products, and the level of targeted, mechanized harvesting is quite high [3–7]. However, there is an extreme lack of research on harvesting machinery for jujubes, especially for dwarf plants and dense planting modes. Nevertheless, the general technology and equipment in the field of forest fruit harvesting still provide valuable references for the development of mechanization of jujube harvesting in China.

At present, China's existing jujube harvesting machinery is mainly divided into two categories according to its working principles: vibration or air suction. Vibrating jujube harvesting machinery exists in various forms, including the robotic vibration shaking trunk type, soft rubber rod rotating pumping type, double toggle drum rotating vibration fruit removal type, and other types [8–11]. Pneumatic suction types include two types: negative-pressure picking and cleaning harvesters and positive- and negative-pressure conversion picking and cleaning harvesters [12–14]. Unfortunately, however, most of these machines are still in the experimental stage and have not been popularized for large-scale application. In actual production, manual picking is still the main harvesting method, and the popularity of mechanized harvesting equipment is extremely low. Chinese jujube planting widely uses dwarf dense planting modes. The mode of mechanized harvesting equipment needs to be adaptable to stringent requirements. The existing harvesting machinery has difficulty realizing efficient operation in dwarf and densely planted orchards, and it is easy to cause damage to date palms in the operation process. In addition, the harvesting of jujubes is highly seasonal and labor demand is concentrated, while the problem of rural labor shortages has become more and more serious in recent years, making the cost of manual harvesting climb sharply. At the same time, the agronomic requirements of jujube planting, such as tree shape, row spacing, and fruiting position, etc., are poorly adapted to mechanized operations, seriously hindering the large-scale promotion of mechanized harvesting.

Based on the analysis of the above issues and referring to the existing jujube harvesting machinery, this study designed a traction-type fresh jujube harvester for trees. This machine utilizes the principle of double-roller collection. The handheld picking head can flexibly move among the jujube trees to pick jujubes. It also tranches and cleans the jujubes through negative-pressure air flow, thus achieving the collection of fresh jujubes from the trees. Through the operation performance testing of the jujube harvester, its performance parameters were verified.

The traction-type fresh jujube harvester designed in this study innovatively adopts self-adjusting picking rollers, which greatly reduces the rate of damage to the jujubes. It is combined with pneumatic harvesting methods to complete picking and cleaning. It not only solves the problem of fresh jujube harvesting under the dwarfing and dense planting

mode but also reduces the damage to jujube trees. This study provides a reference for research on machinery for picking and harvesting fresh jujubes from trees.

2. Materials and Methods

2.1. Main Planting Patterns and Mechanized Harvesting Requirements

China's jujube industry generally adopts a dwarfing and dense planting mode. Under this mode, jujube trees show the characteristics of short and compact plants and wide row spacing, which greatly facilitates the daily management of the orchard, including fertilization, pruning, pest control, etc. At the same time, it has a significant role in promoting the quality of jujube fruits. Compared with the traditional cultivation mode, the dwarf dense planting mode has outstanding advantages in terms of economic benefits. In this planting mode, the jujube tree spacing is 4 m, row spacing is 5 m, the average tree height is 2.5 m, jujube tree crown width is 3.8 m on average. During the design process of the pneumatic jujube harvester, the characteristics of the dwarfing and dense planting mode were fully considered and relied on, aiming to achieve efficient harvesting of jujubes.

2.2. Basic Parameters of Jujube

Bottle jujube is named because its fruit shape resembles a bottle. Its fruit type is long obovate or cylindrical. The whole fruit includes a small section under the big, the middle waist part is slightly slender, and the long obovate fruit is shaped like a pot or bottle.

2.2.1. Measurement of the Shape and Size of Jujubes

We randomly collected 50 ripe jujube bottles and measured the three-axis dimensions with vernier calipers to obtain the length range, width range, and thickness range of the jujube fruit, and measured its single fruit mass.

2.2.2. Measurement of the Floating Speed of Jujubes

In a study of the levitation velocity of jujubes, adopting an L-shaped pitot tube and DP2000-11(Yueqing Aidebao Instrument Co., Ltd., Yueqing, China, Online purchase) intelligent pressure–velocity–air volume meter. Measurement of flow rate was carried out using the differential pressure method with three-stage measurement. The suspension velocity of jujubes and the suspension velocity of date leaves and other impurities were measured.

2.2.3. Measurement of the Binding Force of Jujubes

In order to investigate the distribution of shedding forces in the jujubes, we randomly selected 50 ripe bottle jujubes. Measurement of the shedding force of the jujubes was carried out with the help of SH-50 N digital display push–pull force gauge. The results showed a wide range of distribution of date shedding force values, extending from 2 N to 9.8 N, and the distribution was correlated with the volume of the jujubes. Among them, the percentage of jujubes with shedding force of 5–7 N was about 50%. After data analysis, was found that the measured values were reasonable, there were no outliers, and they were in line with the characteristics of normal distribution. Based on the above research results, to ensure that the pneumatic jujube harvester can meet the required binding force for all jujubes, considering the range of jujube dropping force comprehensively, the picking force of the pneumatic jujube harvester was designed to be 9.8 N. For specific parameters, please refer to Table 1.

Table 1. Basic material parameters of jujube.

Parameters	Value	Unit
Length	21.12–49.5	mm
Wide	18.72–39.11	mm
Thickness	16.9–32.08	mm
Quality of individual fruits	14–29	g
Floating speed	20.56–25.59	m/s
Binding force	2–9.8	N

3. Overall Design and Working Principle

A schematic diagram of the pneumatic jujube harvester's structure is shown in Figure 1. It includes a self-regulating picking mechanism, telescopic conveying tube, negative pressure generator, clearing mechanism, double-chamber collection box, single door shell, control assembly, generator, traction mobile chassis, and other components. It can be hooked up with a hand-held tractor, four-wheeled tractor, and other power machinery for use. Its key technical parameters are shown in Table 2.

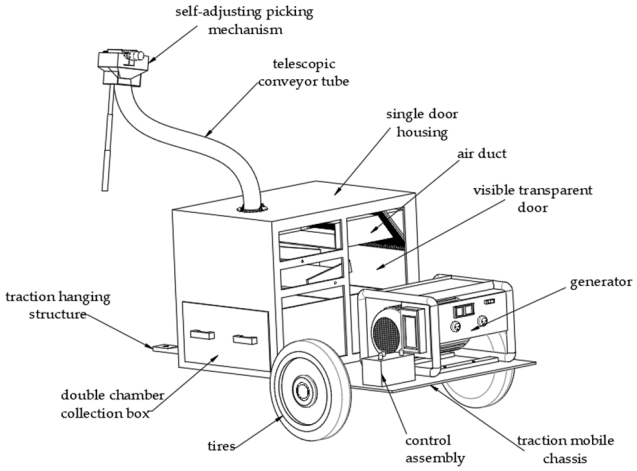


Figure 1. Schematic diagram of the structure of the pneumatic jujube harvesting machine.

Table 2. Key technical parameters of the pneumatic jujube harvester.

Parameters	Value	Unit
Total machine size (L × W × H)	1500 × 800 × 600	mm
Total mass	210	kg
Matched power	8	kw
Working width	2.5	m

When the pneumatic jujube harvester is working in the field, the main unit and the generator are fixed on the towing mobile chassis and connected to power machinery such as a hand-guided tractor or four-wheel tractor. It is powered by an alternator, and the motor and negative-pressure generator provide power.

When this pneumatic jujube harvester is in operation, the handheld self-adjusting picking head, utilizing negative-pressure suction for assistance, guides the jujubes closer to the rotating picking roller in the opposite direction to complete the picking. The mixture enters the main unit through the telescopic conveying pipe. Due to the expansion of the air duct, the cleaning air velocity decreases. The heavier jujubes fall to the upper cleaning baffle under the effect of gravity and are eventually guided into the jujube collection box through the lower cleaning baffle. Light impurities are carried into the air duct by the airflow and

fall into the impurity collection box through the self-cleaning mechanism, achieving the simultaneous completion of picking and cleaning.

4. Structural Parameter Design of the Pneumatic Jujube Harvester

4.1. Design of Picking Roller

A mature bottle jujube can be approximated as an axisymmetric figure. The axis of symmetry and the position of the fruit stalk coincide with the ruler gauge to measure its shape. The shape of the outline is depicted in a right-angled coordinate system to obtain the longitudinal cross-section along the axis of symmetry of the bottle jujube. The longitudinal section can be approximated as an axisymmetric modified ovoid curve, which is characterized by the introduction of segmentation parameters to achieve the morphology of "narrow at the top and wide at the bottom" while maintaining symmetry [15].

The symmetrical modified ovoid curve is as follows:

$$r(\theta) = a(1 + k\cos\theta)\left(1 + \epsilon \sin^2\theta\right) \tag{1}$$

where a is the radius, mm; k is the shrinkage factor, $0 < k < 1$; ϵ is the expansion coefficient, $\epsilon > 0$; θ is the polar angle.

In order to more accurately match the "long inverted ovoid" character of jujubes, the polar angle range can be divided into the top and bottom regions and assigned different parameters as follows:

$$r(\theta) = \begin{cases} a(1 + k_1\cos\theta) & \text{top region}\left(0 \le |\theta| \le \frac{\pi}{2}\right) \\ a(1 + k_2\cos\theta)(1 + \epsilon \sin^2\theta) & \text{bottom area}\left(\frac{\pi}{2} \le |\theta| \le \pi\right) \end{cases} \tag{2}$$

where k_1 is the top shrinkage factor, $k_1 > 0$; k_2 is the bottom shrinkage factor, $k_2 < k_1$; ϵ is the coefficient of expansion, $\epsilon > 0$.

Figure 2 shows the force conditions of the picking roller and the jujube during the picking process. When the resultant force acting on the jujube is greater than the binding force of the fruit stalk, the fruit stalk breaks and the jujube falls off.

$$F_0 - 2F\cos\alpha = 0 \tag{3}$$

$$\sqrt{{F_f}^2 + {F_v}^2} = \sqrt{F^2} \tag{4}$$

where F_v is the collision force of picking rollers on the jujube, N; F_f is the friction of picking rollers on the jujube, N; F is the combined impact force of picking rollers on the jujube, N; α is the angle between the combined impact force and the vertical direction.

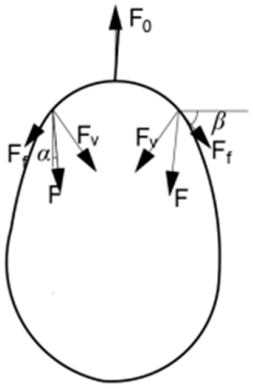


Figure 2. Force analysis diagram of jujube.

The picking mechanism of the pneumatic jujube harvester adopts a double-roller design. Its core working principle is as follows. For power transmission, the picking motor drives two custom-made picking rollers in the shape of jujubes to rotate in opposite directions through the gear transmission. In the picking process, when the tips of the two rotating picking rollers simultaneously touch the top of a jujube, they apply a downward pulling force. For fruit separation, the continuous pulling force eventually exceeds the limit that the fruit stalk can bear, causing it to break and achieving the separation of the jujube from the branch. The picking mechanism consists of three main parts. The jujube-shaped picking roller is customized to the shape of a jujube and is responsible for contact and force application. The transmission gears transmit power and ensure that the two picking rollers rotate in opposite directions. The picking motor provides the power.

Figure 3 shows the structural schematic diagram of the jujube-shaped picking stick. In response to the size and shape of the jujubes, the two picking rollers are designed as concave arc-shaped structures, precisely fitting the upper curve of the jujubes. They can fully accommodate a single jujube body and effectively prevent the jujubes from getting stuck. The surface of the wheel body is wrapped with high-density sponge, and its natural expansion state is suitable for picking jujubes. When encountering jujubes, the sponge is deformed under pressure, providing cushioning protection and reducing the damage rate.

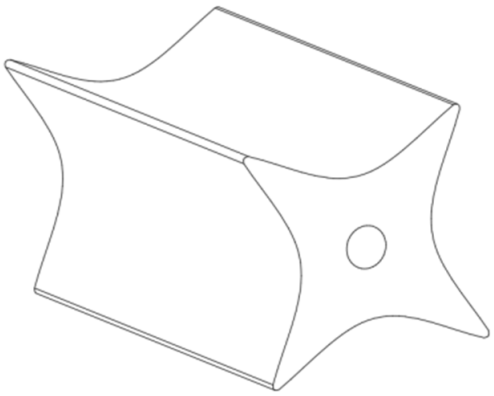


Figure 3. Schematic diagram of the structure of the picking roller.

4.2. Design of Self-Regulating Mechanism

To reduce the rate of damage to fruit during the mechanical harvesting of jujubes and to improve adaptability, an innovative self-regulating double-picking roller mechanism has been designed. Tests show that for jujubes within the range of 20–35 mm in diameter, this mechanism can maintain a constant clamping force, and the breakage rate is reduced by 62.3% compared with traditional fixed mechanisms.

This self-regulating mechanism adopts a three-stage gear transmission system. The motor power forms a first-stage meshing with the gear shaft 2 (z2 = 10) through the pinion (z1 = 11) at the end of the main shaft. The gear shaft 2 drives the large gear 1 (z3 = 30), and then through the idler gear (z4 = 20), it drives the large gear 2 (z5 = 33) to complete the second and third stages of transmission. This design ensures that the two picking rollers achieve precise 1:1 synchronous rotation, with a synchronization error of less than $\pm 1.5^{\circ}$. The structure is shown in Figure 4.

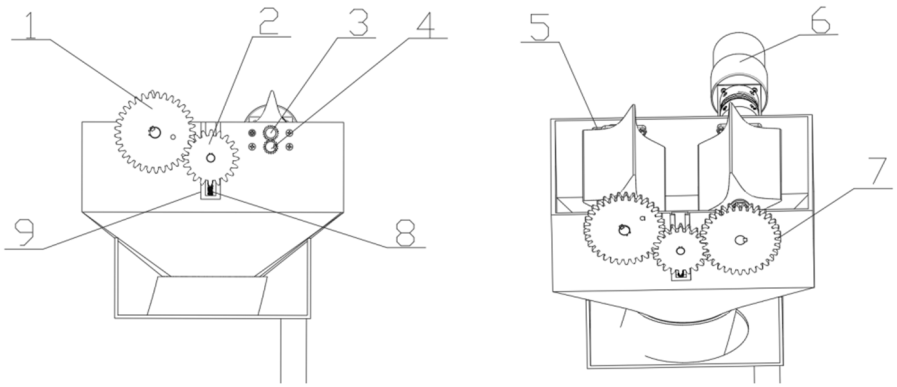


Figure 4. Schematic diagram of the structure of the self-adjusting mechanism. (1) large gear 2; (2) idler pulley; (3) gear shaft 1; (4) gear shaft 2; (5) slide 1; (6) picking motor; (7) large gear 1; (8) spring 1; (9) slide 2.

The calculation of the three-stage transmission ratio is shown in Equation (5):

$$i = \frac{Z_2}{Z_1} \times \frac{Z_4}{Z_3} \times \frac{Z_5}{Z_4} \quad (5)$$

where Z_1 represents the gear shaft 1 teeth; Z_2 represents the gear shaft 2 teeth; Z_3 represents the large gear 1 tooth; Z_4 is the number of idler teeth; Z_5 represents the large gear 2 teeth.

As shown in Figures 4 and 5, the idler wheel is installed on the slide rail 2, which can slide up and down, while the bearing housing of the left picking roller is installed on the slide rail 1, which can slide left and right. The compressed spring 1 under the idler wheel provides elastic force to ensure that the idler wheel meshes with the two large gears for force transmission. The tension spring 2 connecting the two picking roller axles maintains the tension between the wheels. The two springs work together to ensure that the gear set is always engaged. When picking large fruits, the left wheel moves left to increase the wheelbase, and the idler wheel moves upward under the action of spring 1 to compensate, maintaining continuous power transmission. After the fruit passes through, the two spring-driven mechanisms automatically reset to achieve adaptive adjustment of the track.

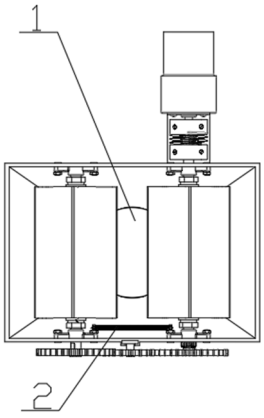


Figure 5. Top view of self-adjusting mechanism: (1) Telescopic conveyor port; (2) Spring 2.

Calculate the tension and elasticity of the spring according to Hooke's Law, as shown in Formula (6):

$$F = kx \quad (6)$$

where F is the spring elasticity/tension; k is the coefficient of restitution, where k1 > k2, N/m; x represents the spring row variable, m.

4.3. Fan Selection

The pneumatic jujube harvester includes a jujube-type picking roller as the main picking part. Negative pressure gas inhalation provides auxiliary work. In the main body of the box, the speed difference in the flow of gas through the jujubes and jujube leaves and other impurities in the suspension completes the process of clearing and selection. The position of the picking head produces a negative-pressure airflow. In this process, avoid large-scale movement of the picking head can reduce labor intensity, and negative-pressure airflow can also avoid the mixture of jujubes and impurities blocking the pipeline.

The model of the fan can be selected according to the air speed, air pressure, and air volume required during the operation of the machine.

Due to the large difference in the suspension speed of jujubes, date leaves, and other impurities, the wind speed and wind pressure required for clearing is small, and the fan design only needs to meet the wind pressure, wind speed, and flow rate required by the conveying pipe and the mouth of the picking head. The wind pressure required by the system is equal to all the pressure loss plus the pressure required by the conveying pipe, i.e., the wind pressure required is equal to the pressure loss of each part. This pressure loss mainly includes dynamic pressure loss, friction pressure loss, and local pressure loss in the conveying pipe.

4.3.1. Wind Speed Selection

The wind speed is determined with reference to the suspension speed of fresh jujubes and the host volume. In order to avoid the clogging of the mixture of jujubes and impurities in the conveying pipe, the design wind speed should be greater than or equal to the suspension speed of the jujubes, and the wind speed is taken as the maximum suspension speed of jujubes, 25 m/s.

4.3.2. Calculation of Wind Pressure

Dynamic pressure loss:

$$P_d = \frac{\rho}{2} v^2 \tag{7}$$

where ρ is the air density, kg/m^3; v is the gas velocity, suspension speed of taking jujube, m/s.

Friction pressure loss, caused by the friction of the airflow against the pipe wall, is calculated according to the Darcy–Weisbach formula, as follows:

$$P_m = f \frac{L}{D} \frac{\rho v^2}{2} \tag{8}$$

where f is the coefficient of friction of the pipes; L is the pipe length, m; D is the pipe inner diameter, m.

Local pressure loss at the suction port is calculated as follows:

$$P_k = (\delta + \sigma_\varphi) \frac{\rho v^2}{2} \tag{9}$$

where δ is the local pressure loss coefficient of suction outlet, δ = 5; $\sigma_\varphi \sigma_\varphi$ is the mixing ratio, harvesting machinery σ_φ = 0.01–0.03, σ_φ= 0.02; v is the inhalation flow rate, m/s; ρ is the dust-to-gas velocity ratio, usually 0.5–0.8, ρ= 0.6.

The total pressure required by the system is as follows:

$$P_d + P_m + P_k \tag{10}$$

4.3.3. Calculation of Air Volume

Pot bottle jujubes have a maximum long axis of 48 mm. The average long axis in approximately 38 mm; in order to reduce the probability of blockage of jujube and impurity mixtures occurring in the conveying pipe conveying process, we selected an inner diameter of 75 mm for the inner wall of the smooth rubber telescopic tube connecting the host computer and the picking head. This operates as a conveying pipe to reduce the friction pressure loss. At the same time, it enables free telescopic bending. The work process is flexible, to minimize the blind picking zone between the jujube tree branches and trunks.

The required airflow is as follows:

$$Q = \frac{AV}{N} \tag{11}$$

where A is the cross-sectional area, m^2; V is the duct air velocity, m/s; N is the sealing factor of the system, 0.8–0.95.

According to the above parameters and formulas, the maximum wind speed required by the pneumatic jujube harvester is 25 m/s, the required wind volume is 576.97 m^3/h, and the required wind pressure is 1574.74 Pa. Two single-phase series-excited high-speed electric fans were selected to meet the demand. The fan model was HLX1600-GS-PE (Shanghai Zhoushui Electric Co., Ltd., Shanghai, China, Online purchase), the fan power was 1600 W, and the rotational speed was 37,000 r/min.

4.4. Design of the Cleaning Device

This separation and impurity removal device uses the difference in the floating speed of jujubes and impurities for cleaning. After the mixture leaves the conveying pipe, it enters the main unit box. The increase in the box space leads to a decrease in wind speed, but it is still higher than the floating speed of impurities. The red dates, being relatively heavy, rolled onto the upper baffle and then rebound through the lower baffle into the red date collection box. The lighter impurities are sucked by the airflow into the inclined automatic cleaning and anti-clogging device for interception and eventually fall into the impurity collection box to achieve separation. The structure is schematically shown in Figure 6.

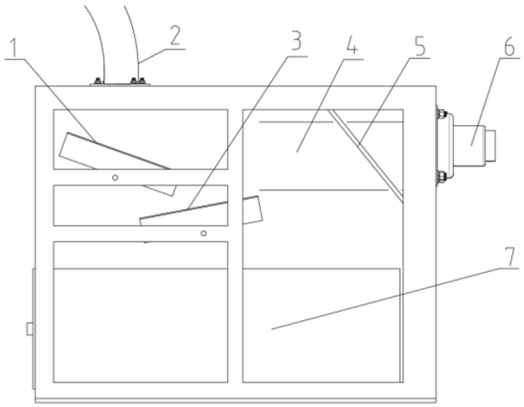


Figure 6. Main view of the clearing mechanism: (1) Upper baffle; (2) Telescopic conveyor tube; (3) Lower baffle; (4) Duct; (5) Mesh belt; (6) Blower; (7) Double-chamber collection box.

To achieve the separation of jujube leaves from red dates, the main unit is designed with a horizontal wind speed of 3.5 m/s (greater than the floating speed of jujube leaves). The mixture has an initial downward velocity when it leaves the tube opening. The light jujube leaves are tossed horizontally and drift to the lower right under the influence of wind speed. Heavy jujubes are less affected by wind speed and mainly move downward, thus achieving effective separation.

This self-cleaning anti-clogging device is driven by a motor to drive the active wheel, which rotates the 45° inclined mesh belt counterclockwise and is equipped with brushes. The rotation of the mesh belt carries impurities away from the high-suction port area of the negative-pressure generator. Some impurities fall off by themselves due to weakened suction or gravity. The residual impurities that fall off automatically are forcibly removed by brushes and eventually fall into the impurity collection box, achieving automatic anti-clogging and impurity removal. Its structure is shown in Figure 7.

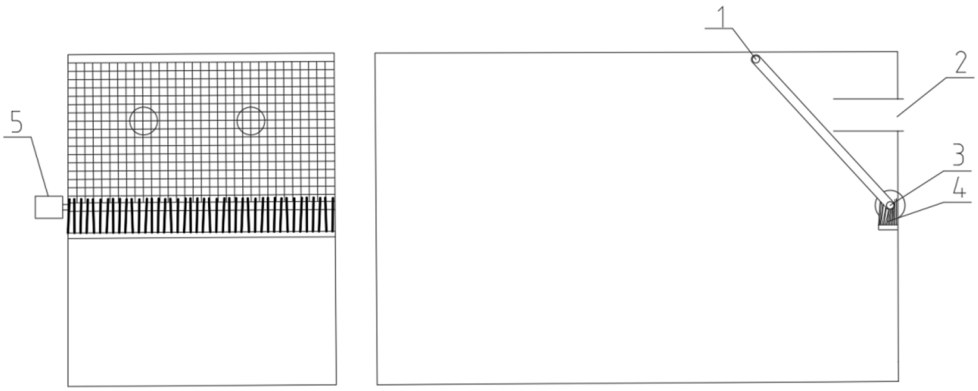


Figure 7. Schematic diagram of self-cleaning mechanism: (1) follower wheel; (2) fan air outlet; (3) active shaft; (4) brush; (5) cleaning motor.

To avoid the movement of the mesh belt on the wind field to produce a greater impact, a 3 cm square hole mesh belt is used, with a wire diameter of d = 1.5 mm, thickness of 1.5 mm, porosity ε = 0.91, length of 50 cm, width of 40 cm, and a speed of u = 0.1 m/s in the horizontal direction 45° to the upper left side. The specific calculations are shown below.

The suction wind speed generated by the suction port channel of the fan is $V_0 = 5$ m/s, and the wind speed is decomposed into components perpendicular and parallel to the blocking net. The calculation process is shown in Equations (12)–(20).

The vertical component is calculated as follows:

$$V_1 = V_0 cos45^\circ \tag{12}$$

The parallel component calculation is as follows:

$$V_2 = V_0 sin45^\circ \tag{13}$$

The breakdown of blocking movement speed perpendicular to the direction of wind speed is as follows:

$$u_1 = ucos45^\circ \tag{14}$$

Parallel to the direction of wind speed, it is as follows:

$$u_2 = usin45^\circ \tag{15}$$

Relative speed in the vertical direction is expressed as follows:

$$V_{rel1} = V_1 + u_1 \tag{16}$$

In the parallel direction, it is as follows:

$$V_{rel2} = V_2 + u_2 \tag{17}$$

Vertical pressure drop is expressed using the porous media pressure drop equation, as follows:

$$\Delta P = \delta \frac{\rho {V_{rel1}}^2}{2}, \delta = \frac{(1-\varepsilon)^2}{\varepsilon} \tag{18}$$

Downstream velocity and turbulence analysis use the following equations.

Vertical velocity after passing the block is expressed as follows:

$$V_1{}' = V_{rel1}\varepsilon - u_1 \tag{19}$$

Neglecting friction in the parallel direction maintains an approximate constant $V_2{}' \approx V_{rel2}$ The synthesis of cleaning speed is as follows:

$$Vcleaning = \sqrt{V_1{}'^2 + V_2{}'^2} \tag{20}$$

Based on the above calculations, it is concluded that the pressure drop during the movement of the single-layer mesh belt is 0.077 Pa, and the cleaning wind speed is 4.74 m/s. When the second layer of the self-cleaning anti-clogging device moves in the reverse direction, the cleaning wind speed is reduced by 10.4% and the air pressure is reduced by 0.154 Pa, as calculated by the same formula. The wind speed is greater than the suspension speed of the jujube leaves, meeting the design requirements.

5. Field Trials

To further verify the performance of the pneumatic jujube harvester, a field experiment was conducted in a jujube forest with an average temperature of 24 °C, jujube trees in the mature stage, a moisture content of 69.65%, an average tree height of 2.2 m, a tree diameter of 14 cm, and a tree crown width of 3.3 m. The trees were 4 to 5 years old, with a tree spacing of 3.8 m and a row spacing of 4.5 m. They were of the short and dense type. The experimental process is shown in Figure 8, below.



Figure 8. Field test.

The impurity rate is the ratio of the mass of impurities to the mass of the mixture, as follows:

$$X = \frac{m_1}{m} \times 100\% \tag{21}$$

where X is the impurity rate,%; m_1 is the impurity mass, kg; m—mass of mixture, kg.

The breakage rate is the ratio of the mass of broken jujubes to the total mass of picked jujubes, as follows:

$$Y = \frac{m_2}{m_0} \times 100\% \tag{22}$$

where Y is the breakage rate, %; m_2 is the broken quality, kg; m_0 is the total mass of jujubes in the collection box, kg.

The leakage rate is the ratio of the mass of unpicked jujubes to the total mass of jujubes, as follows:

$$Z = \frac{m_3}{m_4} \times 100\% \quad (23)$$

where Z is the leakage rate,%; m_3 is the quality of unpicked jujubes, kg; m_4 is the total mass of all jujubes, kg.

To assess harvesting efficiency, the harvester was started to harvest jujubes in the selected operation area. At the end of the operation, all the jujubes in the collection box were weighed and recorded as m_0. The time taken to complete the harvesting operation in the operational area was recorded using a timer t. The time taken to complete the harvesting operation in the operational area was recorded using a timer.

$$W = \frac{m_0}{t} \quad (24)$$

where W is the harvesting efficiency, kg/h; m_0 is the total mass of jujubes in the collection box, kg; t is the time spent on harvesting operations, h.

In the course of the field trials, single-factor and multi-factor tests were carried out on the pneumatic jujube harvester with suction wind speed, picking roller rotational speed, and upper and lower cleaning baffle angles as test factors, and leakage picking rate, breakage rate, impurity content rate, and picking efficiency as evaluation indexes.

5.1. One-Factor Test

The picking roller's rotational speed directly affects the picking efficiency. The upper and lower cleaning baffle angle and wind speed directly affect the rate of impurities. In order to determine whether the pneumatic jujube harvester is suitable for the working parameters, we selected four test factors. The material characteristics and suspension characteristics of jujubes and impurities and the appropriate amplification determine the suction wind speed and the upper and lower cleaning baffle angles. According to the current artificial picking efficiency, and to determine the picking roller rotational speed level, four test factors are shown in Table 3.

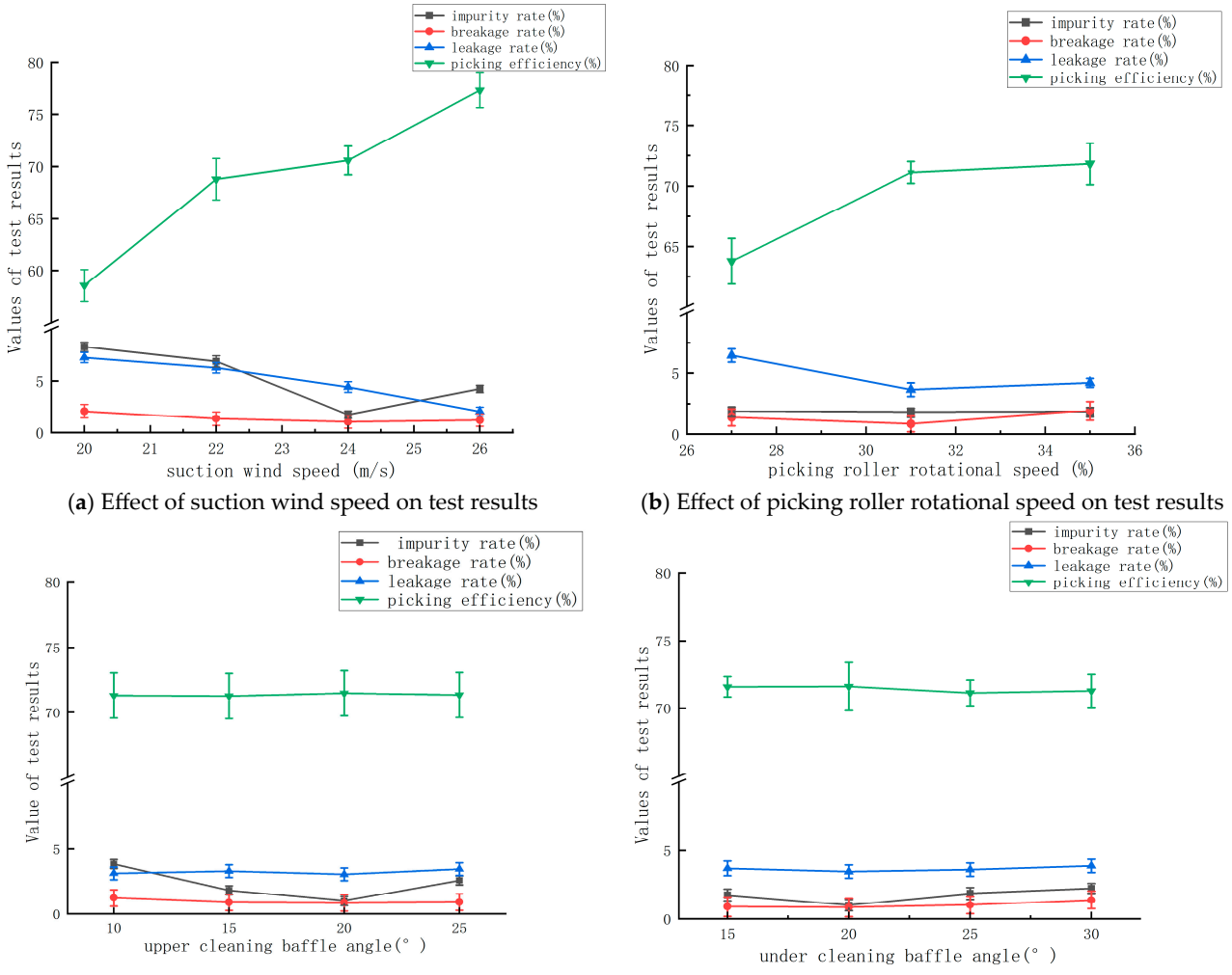
Table 3. Key technical parameters of pneumatic jujube harvester.

Suction Wind Speed m/s	Picking Roller Rotational Speed r/min	Upper Cleaning Baffle Angle°	Under Cleaning Baffle Angle°
20	27	10	10
22	31	15	15
24	35	20	20
26		25	25

For the single-factor picking test, the other three factors except the variable factors were taken as fixed values. The suction wind speed was selected, the picking roller rotational speed and the upper and lower cleaning baffle angles were fixed values. The picking roller rotational speed was selected, and the suction wind speed and the upper and under cleaning baffle angles were fixed values. The upper cleaning baffle angle was selected, and the suction wind speed, the picking roller rotational speed, and the lower cleaning baffle angle were fixed values. The lower cleaning baffle angle was selected, and the suction wind speed, the picking roller rotational speed, and the upper cleaning baffle angle were fixed

values. The four test factors were taken as fixed values of 24 m/s, 31 r/min, 15° and 20°, respectively.

During the test, we turned on the power supply, adjusted the parameters to the test level, and held the picking head to select an unpicked jujube tree to start the test. Each group of picking tests lasted for two to three minutes. After the test, we turned off the power supply, and manually counted the number of unsuccessfully picked jujubes. We opened the double-chamber collection box to weigh the jujubes and the impurities. We manually checked the breakage of jujubes and their classification. Weighing and recording of test data were repeated three times to obtain average values to reduce the error. The test results are shown in Figure 9.



(**a**) Effect of suction wind speed on test results

(**b**) Effect of picking roller rotational speed on test results

(**c**) Effect of upper cleaning baffle angle on test results

(**d**) Effect of under cleaning baffle angle on test results

Figure 9. Results of the one-factor test.

The experimental results show that, with the increase in suction wind speed, the picking efficiency gradually increased, the impurity rate and the breakage rate decreased first and then increased, reaching their lowest at 24 m/s, and the leakage rate gradually decreased. With the increase in picking roller rotational speed, the picking efficiency and the impurity rate gradually increased, and the breakage rate and the leakage rate decreased first and then increased. With the gradual increase in the angle of the upper baffle plate, the impurity rate decreased first and then increased, and the rest of the changes were not significant. With the gradual increase in the angle of the lower baffle, the breakage rate gradually increased, the impurity content decreased first and then increased, and the rest of the changes were not obvious.

5.2. Performance Optimization Regression Test

Through the single-factor test and test prototype pretest program, in order to carry out scientific and effective experiments, we explored the interaction between multiple factors, looking for the best performance parameters of the jujube harvester. We used a Box–Benken center combination experimental design to carry out the four-factor three-level regression test. For the suction wind speed 20 m/s, the rate of impurity content, leakage rate, picking efficiency were not ideal; only the breakage rate is lower. The difference at 22 m/s was only 0.2%, and the comprehensive effect was not obvious; when the upper and lower baffle angles were 10° the breakage rate and the impurity rate were not the smallest. With an increase in the angle there was a tendency for these to reduce. Therefore, according to the relationship between the picking parameters and picking indicators, we selected the more suitable picking parameters for the regression test. The test factors and levels are shown in Table 4.

Table 4. Coding table for the levels of the test factors.

	Considerations			
Encodings	**Suction Wind Speed/A (m/s)**	**Picking Roller Rotational Speed/B (r/min)**	**Upper Cleaning Baffle Angle/C (°)**	**Lower Cleaning Baffle Angle/D (°)**
−1	22	27	15	15
0	24	31	20	20
1	26	35	25	25

The test program and response values are shown in Table 5.

Table 5. Results of the test program and response values.

Serial Number	**Level of Factors**				**Response Value**			
	A	**B**	**C**	**D**	**X (%)**	**Y (%)**	**Z (%)**	**W (kg/h)**
1	1	0	0	−1	4.25	1	2.09	77.1
2	1	0	−1	0	5.16	1.01	2.15	76.39
3	0	0	−1	−1	1.03	1.31	6.34	61.98
4	−1	0	0	−1	7.77	0.9	4.03	68.97
5	0	−1	0	−1	1.14	1.32	6.21	63.52
6	−1	0	−1	0	5.89	1.39	8.36	60.38
7	0	1	0	−1	2.69	1.8	4.39	68.28
8	1	−1	0	0	3.47	1.02	1.62	77.84
9	−1	−1	0	0	5.78	0.91	4.31	69.37
10	0	0	1	−1	1.05	1.81	4.21	69.97
11	0	−1	−1	0	1.07	0.79	3.06	71.39
12	0	1	−1	0	2.61	0.83	3.67	70.39
13	0	0	0	0	1.91	0.82	3.91	72.48
14	0	0	0	0	1.16	0.8	3.48	70.97
15	1	1	0	0	3.49	1.48	4.17	67.08
16	0	0	0	0	1.89	1.3	6.48	63.45
17	1	0	1	0	3.53	1.96	3.41	75.38
18	0	−1	1	0	3.47	1.3	6.31	63.47
19	0	1	1	0	1.05	0.81	3.81	72.24
20	−1	1	0	0	6.96	0.9	4.26	68.31
21	−1	0	1	0	5.94	0.92	4.47	67.14
22	0	0	−1	1	1.8	0.82	3.67	71.08
23	1	0	0	1	3.36	1.01	1.94	78.61
24	0	−1	0	1	1.15	1.82	4.71	67.61
25	−1	0	0	1	5.91	1.87	5.06	68.41
26	0	1	0	1	1.86	1.81	4.29	68.69
27	0	0	1	1	2.72	0.83	3.62	71.57

Design-Expert 13.0 was utilized to carry out multivariate fitting of the data in the table and then obtain the regression equations of the effects of suction wind speed, picking roller rotational speed, upper cleaning baffle angle, and lower cleaning baffle angle on the impurity rate, breakage rate, leakage rate, and picking efficiency, to carry out the significance test, and then finally, to carry out the response surface analysis of the experimental indexes of each factor to derive the optimal experimental parameters for the jujube harvester.

5.2.1. Impurity Rate Regression Analysis and Significance Test

The experimental data were analyzed using Design-Expert 13.0 software and the results of the significance test of the regression equation are shown in the table. For the impurity rate model X, the significant level p-value is less than 0.0001 and the fit is highly significant ($p < 0.01$). The p-value of the misfit term is 0.111, and the misfit term is not significant at a level greater than 0.05. The coefficient of determination of the regression equation, R^2 = 0.9773, indicates that more than 97% of the evaluation indexes can be explained by the change of the mathematical model, and the regression equation of the effect of each test factor on the impurity rate is obtained as shown in Equation (25):

$$\begin{aligned} X = \; & 1.09 - 1.25A - 0.06B + 0.4792C + 0.0583D + 0.005AB + 0.025AC \\ & -0.0125AD - 0.1875BC - 0.0025BD + 3.61A^2 + 0.562B^2 + 1.31C^2 - 0.0862D^2 \end{aligned} \quad (25)$$

From the results of ANOVA, it can be seen that the p-values of suction wind speed A, upper cleaning baffle angle C, and square terms A^2 and C^2 in the model of the impurity rate are <0.01, which is highly significant. Thus, the degree of influence of each factor on the impurity rate, from big to small, is the suction wind speed A, upper cleaning baffle angle C, picking roller rotational speed B, and the angle of the lower baffle D. The ANOVA results are shown in Table 6.

Table 6. Analysis of variance of impurity rate regression.

Source	Impurity Rate				
	Sum of Squares	**df**	**Mean Square**	**F-Value**	***p*-Value**
Model	107.74	14	7.7	312.77	<0.0001
A	18.73	1	18.73	760.99	<0.0001
B	0.0432	1	0.0432	1.76	0.2098
C	2.76	1	2.76	111.97	<0.0001
D	0.0408	1	0.0408	1.66	0.222
AB	0.0001	1	0.0001	0.0041	0.9502
AC	0.0025	1	0.0025	0.1016	0.7554
AD	0.0006	1	0.0006	0.0254	0.876
BC	0.1406	1	0.1406	5.72	0.0341
BD	0	1	0	0.001	0.9751
CD	0	1	0	0	1
A^2	69.41	1	69.41	2820.76	<0.0001
B^2	0.0169	1	0.0169	0.6858	0.4238
C^2	9.08	1	9.08	369.13	<0.0001
D^2	0.0397	1	0.0397	1.61	0.2282
Residual	0.2953	12	0.0246		
Lack of Fit	0.2884	10	0.0288	8.4	0.111
Pure Error	0.0069	2	0.0034		
Cor Total	108.04	26			

5.2.2. Regression Analysis of Breakage Rate and Significance Test

For the breakage rate model Y, the significant level p-value is less than 0.0001 and the fit is highly significant ($p < 0.01$). The p-value of the misfit term is 0.5791, which is greater than

0.05. The misfit term is not significant, and the coefficient of determination of the regression equation is R^2 = 0.9997, which indicates that more than 99% of the evaluation indexes can be explained by the change of the mathematical model. The regression equations for the effect of each test factor on the impurity rate are obtained as shown in Equation (26):

$$\begin{aligned} Y = \; & 0.8 + 0.0458A + 0.2575B + 0.015C + 0.0167D + 0.0075AB - 0.015AC \\ & + 0.1567A^2 + 0.7492B^2 + 0.0254C^2 + 0.0729D^2 \end{aligned} \quad (26)$$

From the ANOVA results, it can be seen that in the breakage rate model, the *p*-values of the square terms A^2, B^2, C^2, and D^2 of the suction wind speed A, picking roller rotational speed B, upper cleaning baffle angle C, and under cleaning baffle angle D are <0.01, indicating a highly significant effect on the breakage rate, and the degree of influence of each factor on the breakage rate from the largest to the smallest is the picking roller rotational speed A, the suction wind speed B, the lower cleaning baffle angle D, and the upper cleaning baffle angle C. The results of the analysis of variance (ANOVA) indicate that the breakage rate model has a highly significant effect on the breakage rate. The ANOVA results are shown in Table 7.

Table 7. Regression ANOVA for breakage rate.

Source	Breakage Rate				
	Sum of Squares	**df**	**Mean Square**	**F-Value**	***p*-Value**
Model	4.22	14	0.3013	1132.67	<0.0001
A	0.0252	1	0.0252	94.78	<0.0001
B	0.7957	1	0.7957	2991.57	<0.0001
C	0.0027	1	0.0027	10.15	0.0078
D	0.0033	1	0.0033	12.53	0.0041
AB	0.0002	1	0.0002	0.8460	0.3758
AC	0.0009	1	0.0009	3.38	0.0907
AD	0.0000	1	0.0000	0.0000	1.0000
BC	0.0000	1	0.0000	0.0000	1.0000
BD	0.0000	1	0.0000	0.0000	1.0000
CD	0.0000	1	0.0000	0.0000	1.0000
A^2	0.1309	1	0.1309	492.17	<0.0001
B^2	2.99	1	2.99	11,254.32	<0.0001
C^2	0.0034	1	0.0034	12.95	0.0037
D^2	0.0284	1	0.0284	106.61	<0.0001
Residual	0.0032	12	0.0003		
Lack of Fit	0.0030	10	0.0003	2.99	0.2764
Pure Error	0.0002	2	0.0001		
Cor Total	4.22	26			

5.2.3. Leakage Rate Regression Analysis and Significance Test

For the leakage rate model Z, the significant level *p*-value is less than 0.0001 and the fit is highly significant ($p < 0.01$). The *p*-value of the misfit term is 0.7745, greater than 0.05; the misfit term is not significant. The regression equation coefficient of determination R^2 = 0.9609, which indicates that more than 96% of the evaluation indexes can be explained by the change of mathematical model. The regression equation of the effect of each test factor on the impurity rate is as shown in Equation (27):

$$\begin{aligned} Z = \; & 3.45 - 1.26A - 0.9833B - 0.0442C + 0.333D + 0.635AB + 0.0725AC - 0.12AD \\ & + 0.0675BC + 0.1575BD - 0.0725CD - 0.3113A^2 + 1.95B^2 \\ & + 0.0638C^2 + 0.04D^2 \end{aligned} \quad (27)$$

From the results of the ANOVA, it can be seen that in the leakage rate model, the *p*-values of suction wind speed A, picking roller rotational speed B, interaction term AB, and square terms A^2, B^2 are <0.05, indicating a significant effect on the leakage rate. The upper and lower baffles are not involved in the picking session and do not affect the leakage rate, which is consistent with the design. The degree of influence on the leakage rate is greatest for the picking roller rotational speed B, followed by the suction wind speed A. The ANOVA results are shown in Table 8.

Table 8. Regression ANOVA for leakage rate.

Source	Leakage Rate				
	Sum of Squares	**df**	**Mean Square**	**F-Value**	***p*-Value**
Model	59.62	14	4.26	46.59	<0.0001
A	19.03	1	19.03	208.14	<0.0001
B	11.6	1	11.6	126.93	<0.0001
C	0.0234	1	0.0234	0.2561	0.622
D	0.0133	1	0.0133	0.1459	0.7092
AB	1.61	1	1.61	17.64	0.0012
AC	0.021	1	0.021	0.23	0.6401
AD	0.0576	1	0.0576	0.6301	0.4427
BC	0.0182	1	0.0182	0.1994	0.6632
BD	0.0992	1	0.0992	1.09	0.318
CD	0.021	1	0.021	0.23	0.6401
A^2	0.5167	1	0.5167	5.65	0.0349
B^2	20.23	1	20.23	221.28	<0.0001
C^2	0.0217	1	0.0217	0.2371	0.6351
D^2	0.0085	1	0.0085	0.0934	0.7652
Residual	1.1	12	0.0914		
Lack of Fit	0.8143	10	0.0814	0.5763	0.7745
Pure Error	0.2826	2	0.1413		
Cor Total	60.72	26			

5.2.4. Picking Efficiency Regression Analysis and Significance Test

For the picking efficiency model W, the significant level *p*-value is less than 0.0001 and the fit is highly significant ($p < 0.01$). The *p*-value of the misfit term is 0.2362, greater than 0.05; the misfit term is not significant. The regression equation coefficient of determination $R^2 = 0.9413$, which indicates that more than 94% of the evaluation indexes can be explained by the change of mathematical model. The regression equation for the effect of each experimental factor on the impurity rate is as shown in Equation (28):

$$\begin{aligned} W = \; & 71.53 + 4.15A + 3.21B - 0.17C - 0.1033D + 0.0675AB - 0.3425AC + 0.365AD \\ & -0.1075BC - 0.975BD - 0.055CD + 1.63A^2 - 5.47B^2 - 0.2221C^2 \\ & -0.0496D^2 \end{aligned} \quad (28)$$

From the ANOVA results, it can be seen that in the picking efficiency model, the $p < 0.01$ of suction wind speed A, picking roller rotational speed B, square terms A^2 and B^2, indicate that the effect on picking efficiency is highly significant, and the angle of the upper and lower baffles does not affect the picking efficiency, which is consistent with the design. The degree of influence of the test factors on the picking efficiency is greatest for the speed of the picking roller A, followed by suction wind speed B. The ANOVA results are shown in Table 9.

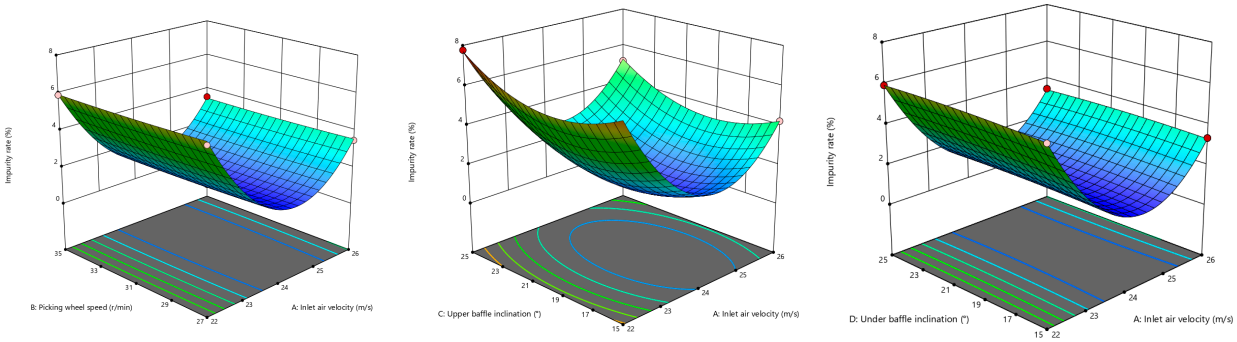
Table 9. Picking efficiency regression ANOVA.

Source	Picking Efficiency				
	Sum of Squares	**df**	**Mean Square**	**F-Value**	***p*-Value**
Model	573.65	14	40.98	30.8	<0.0001
A	206.84	1	206.84	155.5	<0.0001
B	123.26	1	123.26	92.67	<0.0001
C	0.3468	1	0.3468	0.2607	0.6189
D	0.1281	1	0.1281	0.0963	0.7616
AB	0.0182	1	0.0182	0.0137	0.9088
AC	0.4692	1	0.4692	0.3528	0.5636
AD	0.5329	1	0.5329	0.4006	0.5386
BC	0.0462	1	0.0462	0.0348	0.8552
BD	3.8	1	3.8	2.86	0.1167
CD	0.0121	1	0.0121	0.0091	0.9256
A^2	14.13	1	14.13	10.63	0.0068
B^2	159.41	1	159.41	119.84	<0.0001
C^2	0.263	1	0.263	0.1978	0.6645
D^2	0.0131	1	0.0131	0.0099	0.9226
Residual	15.96	12	1.33		
Lack of Fit	15.12	10	1.51	3.61	0.2362
Pure Error	0.8373	2	0.4186		
Cor Total	589.61	26			

5.3. Performance Optimization Regression Test Analysis

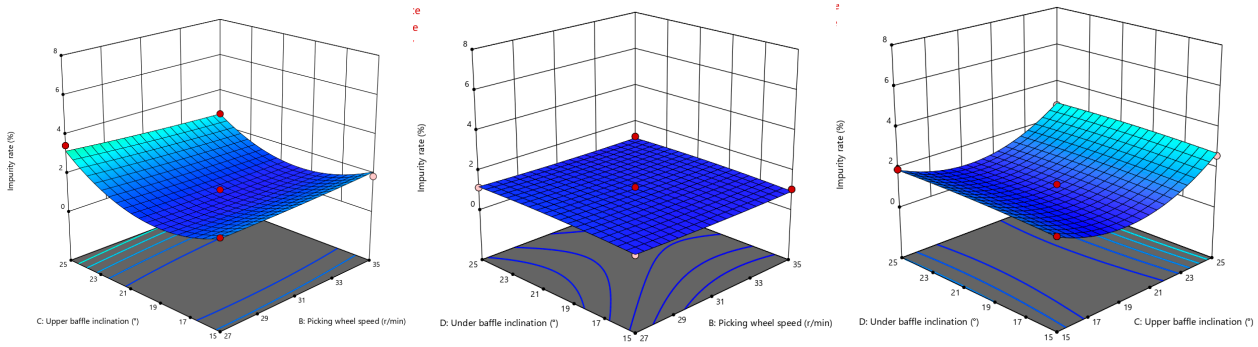
5.3.1. Effect of Factors on Impurity Rate (X)

Figure 10a indicates that when the upper and under baffles are at zero level, the suction wind speed and picking roller rotational speed impact the impurity rate. According to the graph, it can be seen that the interaction effect is not large. When the suction wind speed is constant and the picking roller rotational speed increases, the impurity rate has an an increasing trend, but the impact is not large. When the picking roller rotational speed is unchanged and the suction wind speed decreases and then increases, the impact is more significant, and the two interact with each other. When the two interact, the suction wind speed plays a decisive role in the impurity rate.



(**a**) (**b**) (**c**)

Figure 10. *Cont.*



(**d**) (**e**) (**f**)

Figure 10. Response surface analysis of the effect of each test factor on impurity rate. (**a**) Suction wind speed and picking roller speed. (**b**) Suction wind speed and upper cleaning baffle angle. (**c**) Suction wind speed and lower cleaning baffle angle. (**d**) Picking roller speed and upper cleaning baffle angle. (**e**) Picking roller speed and lower cleaning baffle angle. (**f**) Upper cleaning baffle angle and lower cleaning baffle angle.

Figure 10b reflects the mutual influence of the suction wind speed and the upper baffle angle on the impurity rate when both the rotational speed of the picking roller and the angle of the lower baffle are at zero level. It can be seen from the graph that the interaction has a significant impact. When the suction wind speed and the angle of the upper baffle are at a medium level, the impurity rate drops below 1%. The results show that under the interactive influence of the suction port wind speed and the angle of the upper baffle, taking the suction port wind speed as the test factor, there is a decisive effect on the impurity rate. From the perspective of monotonicity, as the angle of the upper baffle keeps increasing, the impurity rate shows a trend of first decreasing and then increasing. With the continuous increase in the suction port wind speed, the impurity rate shows a trend of first decreasing and then increasing.

Figure 10c reflects when the picking roller rotational speed and the upper cleaning baffle angle are at zero level, the suction wind speed and the lower cleaning baffle angle interact with an effect on the impurity rate, but according to the graph, it can be seen that the interaction effect is not large. When the suction wind speed remains unchanged and the lower cleaning baffle angle continues to increase, the impurity rate first decreases. In the increasing trend, a single effect is more obvious; when the lower cleaning baffle angle remains unchanged and the suction wind speed increases, the impurity rate first decreases and then increases. The single effect is more obvious when the lower cleaning baffle angle remains unchanged and the suction wind speed increases. When the angle of the lower baffle is kept constant, with the increasing suction wind speed, the impurity rate tends to decrease first and then increase.

Figure 10d shows the interaction between the picking roller rotational speed and the angle of the upper baffle on the impurity rate, when the suction wind speed and the angle of the lower baffle are at zero level. When the picking roller rotational speed is kept constant, as the angle of the upper baffle continues to increase, the impurity rate appears to first to decrease and then increase; when the angle of the upper baffle stays the same, as the picking roller rotational speed increases, the impurity rate follows a decreasing trend, but the interaction between the two is less important for the impurity rate and the interaction between the two effects on the impurity rate is small.

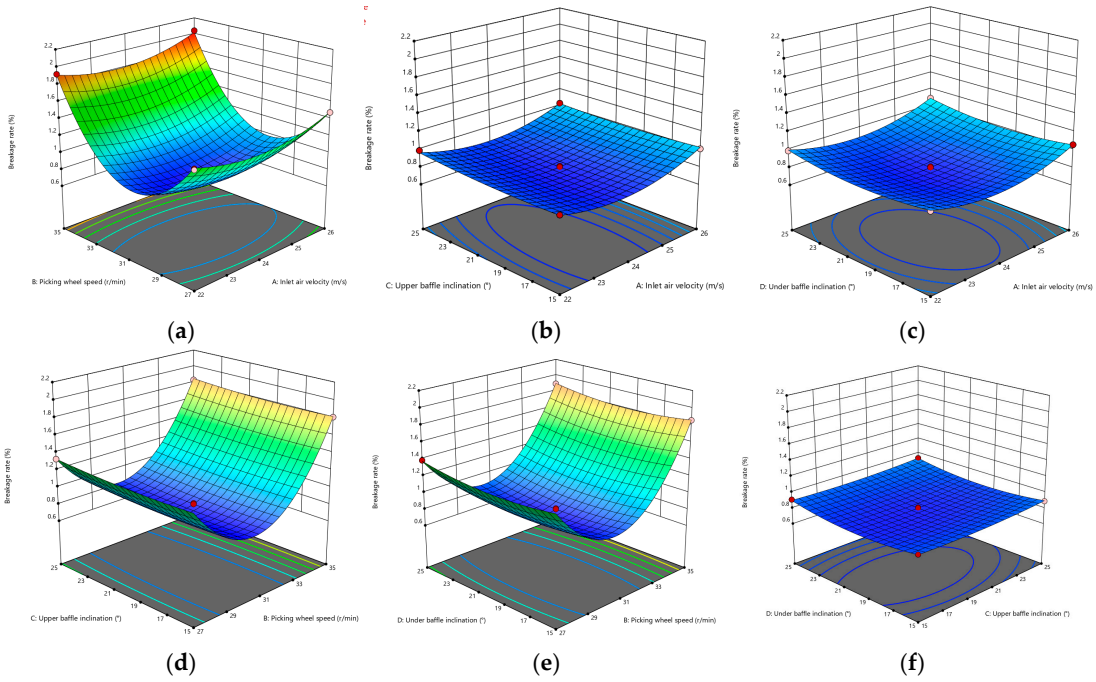
Figure 10e shows that the influence of picking roller rotational speed and lower cleaning baffle angle on the impurity rate is very small.

Figure 10f shows the effect of upper and lower cleaning baffle angle on the impurity rate when the suction wind speed and picking roller rotational speed are at zero level. From

the figure, it can be seen that under the interaction of the two, the upper cleaning baffle angle plays a decisive role in the influence of the impurity rate; from the point of view of monotonicity, with the increasing angle of the lower baffle, there is a slight tendency for the impurity rate to decrease and then increase, although the change is not obvious. When the angle of the lower baffle is kept constant, with the increase in the angle of the upper baffle, the impurity content decreases first and then increases, and the change is more obvious.

5.3.2. Effect of Factors on Breakage Rate (Y)

Figure 11a indicates the effect of the suction wind speed and picking roller rotational speed on the breakage rate when the upper and under baffles are at zero level. From the shape of the graph, it can be seen that in the interaction between the two, the picking roller rotational speed has a decisive effect on the breakage rate. At a picking roller rotational speed of 31 r/min and suction wind speed of 24 m/s, the breakage rate is the lowest, down to less than 1%. From the monotonic point of view, with the increase in the picking roller rotational speed, the breakage rate follows a trend of decreasing first and then increasing; with the increase in suction wind speed, the breakage rate follows a trend of decreasing first and then increasing.



(**a**) (**b**) (**c**)

(**d**) (**e**) (**f**)

Figure 11. Response surface analysis of each test factor on breakage rate. (**a**) Suction wind speed and picking roller speed. (**b**) Suction wind speed and upper cleaning baffle angle. (**c**) Suction wind speed y and lower cleaning baffle angle. (**d**) Picking roller speed and upper cleaning baffle angle. (**e**) Picking roller speed and lower cleaning baffle angle. (**f**) Upper cleaning baffle angle and lower cleaning baffle angle.

Figure 11b,c reflects mutual influence of the suction wind speed and the upper and lower cleaning baffle angle on the breakage rate. According to the response surface, it can be seen that the interaction of the two has little influence on the breakage rate, which is slightly affected only by the suction wind speed. Overall, with the increasing suction wind speed, the breakage rateshows a trend of first decreasing and then increasing, because the upper and under baffle plate surface are glued to the high-density sponge, to avoid the damage to the jujube, and the design of the mechanical structure is consistent.

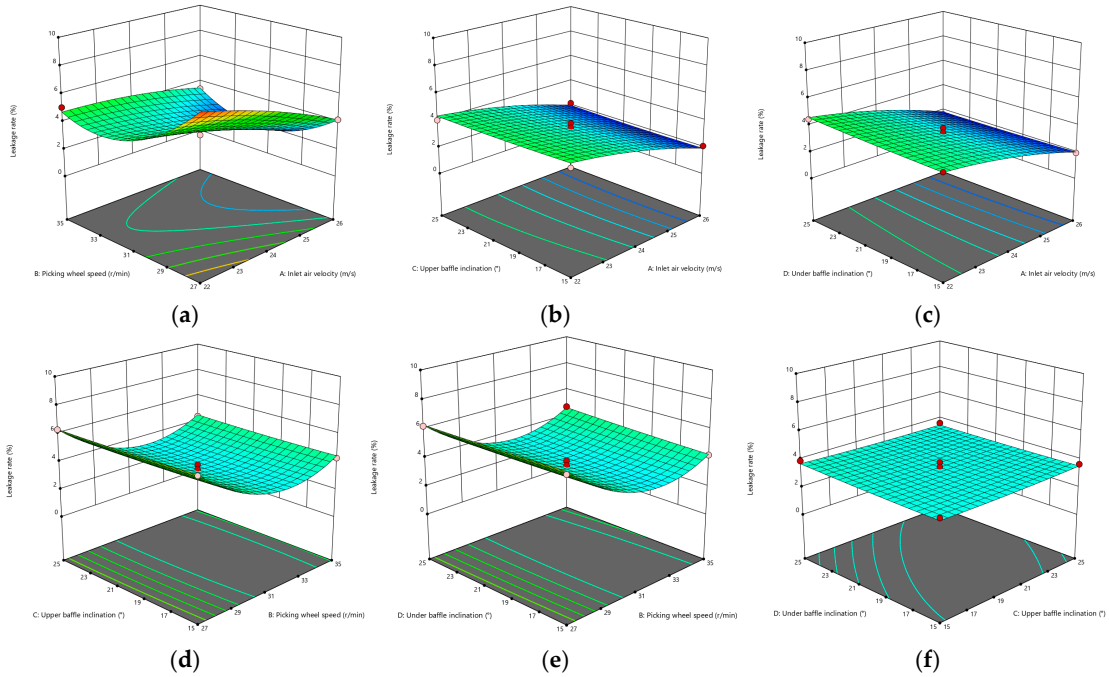
Figure 11d,e indicate the mutual influence of picking roller rotational speed and upper and lower cleaning baffle angles on the breakage rate. According to the response surface, it

can be seen that the interaction of the two has little effect on the breakage rate. The effect of the picking roller rotational speed is more pronounced; in the interaction of the two, the picking roller rotational speed plays a decisive role in the impact of the breakage rate, and the design of the mechanical structure is consistent.

Figure 11f shows the effect of the upper and lower cleaning baffle angles on the breakage rate when the suction wind speed and the picking roller rotational speed are at the zero level. According to the response surface, it can be seen that the interaction between the two has a small effect on the breakage rate. Regarding monotonicity, with the increasing angle of the lower baffle, the breakage rate follows a decreasing and then increasing trend; with the increasing angle of the upper baffle, there is a slight decreasing and then increasing trend in the breakage rate, but the changes are neither significant nor obvious.

5.3.3. Effect of Factors on Leakage Rate (Z)

Figure 12a represents the interaction effect of suction wind speed and picking roller rotational speed on the leakage rate when both upper and lower baffles are at zero level. According to the surface morphology, the leakage rate is significantly affected by the interaction effect and reaches the minimum at the middle level of the picking roller rotational speed. The leakage rate appears to decrease and then increase with the increase in the picking roller rotational speed; the suction wind speed's impact on the leakage rate decreases with the increase in the suction wind speed, and reaches its minimum at the maximum suction wind speed. The minimum value is reached when the suction wind speed is at its maximum.



(**a**) (**b**) (**c**)

(**d**) (**e**) (**f**)

Figure 12. Response surface analysis of leakage rate by test factors. (**a**) Suction wind speed and picking roller speed. (**b**) Suction wind speed and upper cleaning baffle angle. (**c**) Suction wind speed and lower cleaning baffle angle. (**d**) Picking roller speed and cleaning baffle angle. (**e**) Picking roller speed and lower cleaning baffle angle. (**f**) Upper cleaning baffle angle and lower cleaning baffle angle.

Figure 12b,c show the surface morphology; it can be seen that the effect of the suction wind speed and upper and lower cleaning baffle angle on the leakage rate of the interaction is not significant, according to the curvature of the response surface. The leakage rate has no interaction effect, consistent with the design of the mechanical structure.

Figure 12d,e also show the surface morphology; it can be seen that the effect of the picking roller rotational speed and the upper and lower cleaning baffle angle on the leakage rate of the mutual influence is not significant. The picking roller rotational speed is the single factor affecting the trend. As the picking roller rotational speed continues to increase, the leakage rate first decreases and then increases. The trend of the leakage rate in the middle of the horizontal position of the graph is the lowest, and the design of the mechanical structure is consistent.

The surface morphology shown in Figure 12f shows that the effect of the upper and lower cleaning baffle angle on the leakage rate of mutual influence is not significant. Because neither of these are not involved in the picking process, they do not affect the leakage rate.

5.3.4. Effect of Factors on Harvesting Efficiency Rate (W)

Figure 13a represents the mutual influence of suction wind speed and picking roller rotational speed on picking efficiency when both upper and lower baffles are at zero level. According to the surface morphology, the picking efficiency is significantly affected by the interaction effect of the two. The degree of change in the graph indicates that the influence of the two on the picking efficiency is larger when the suction wind speed is 22 m/s, and the picking roller rotational speed is 27 r/min, with the lowest picking efficiency about 60 kg/h. From the monotonicity point of view, the picking efficiency gradually increases with the increase in suction wind speed, but it increases first and then decreases with the increase in suction wind speed.

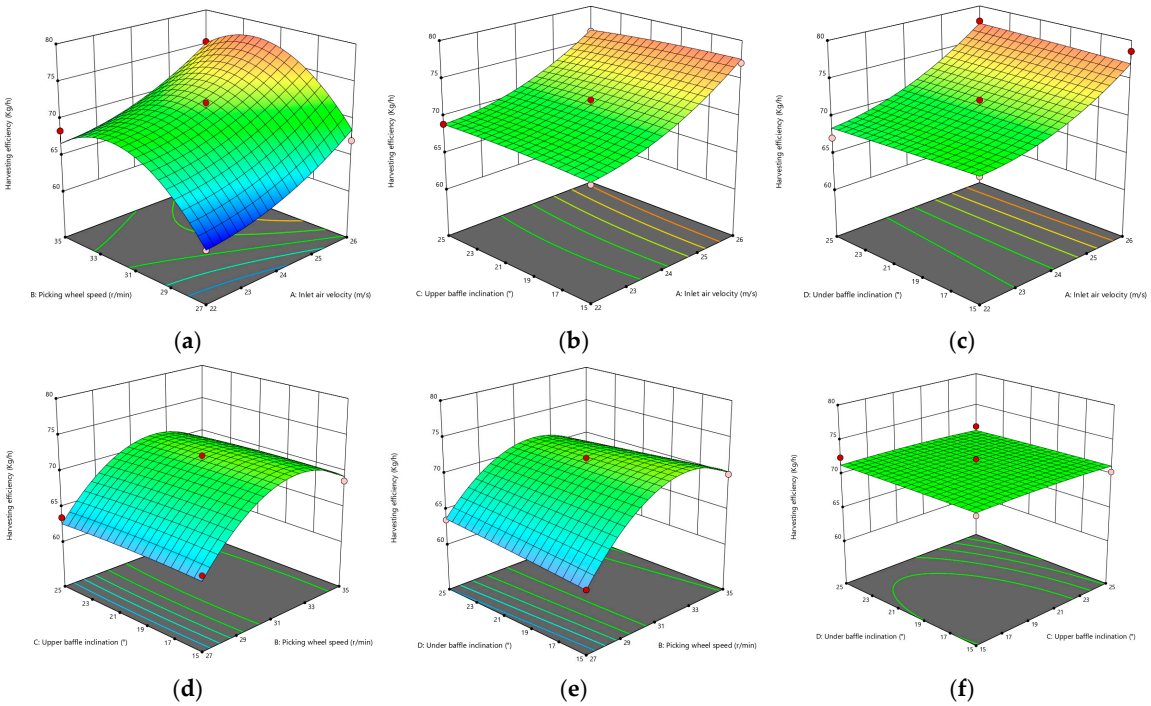


Figure 13. Response surface analysis of experimental factors' effects on harvesting efficiency. (**a**) Suction wind speed and picking roller speed. (**b**) Suction wind speed and upper cleaning baffle angle. (**c**) Suction wind speed and lower cleaning baffle angle. (**d**) Picking roller speed and upper cleaning baffle angle. (**e**) Picking roller speed and lower cleaning baffle angle. (**f**) Upper cleaning baffle angle and lower cleaning baffle angle.

Figure 13b,c show that the effects of suction wind speed and upper and lower cleaning baffle angle on the picking efficiency of the interaction are not significant. According to the curvature of the response surface, only the suction wind speed has an influence. Upper

cleaning baffle angle and lower cleaning baffle angle are no interaction with the efficiency of picking, and the design of the mechanical structure is consistent.

In Figure 13d,e, the surface morphology can also be seen. The effect of picking roller rotational speed and upper and lower cleaning baffle angle on the picking efficiency of the mutual influence is not significant. The picking roller rotational speed is the single factor contributing to the trend; as the picking roller rotational speed continues to increase, the picking efficiency first decreases and then increases. The trend in the middle of the horizontal position of the picking efficiency graph is the largest, and the design of the mechanical structure is consistent.

In Figure 13f, the surface morphology shows that the effect of the upper and lower cleaning baffle angles on the picking efficiency of the interaction is not significant; because neither are involved in the picking process, they do not affect the picking efficiency.

5.4. Optimal Parameter Combination and Validation Test

Based on the optimization module in Design-Expert, the optimal solution of the mathematical model was found through the best combination of parameters, which were provided as follows: suction wind speed 25.198 m/s, picking roller rotational speed 31.168 r/min, upper cleaning baffle angle −18.93°, lower cleaning baffle angle 19.414°. The predicted values of the model were as follows: impurity content 1.586%, breakage rate 0.895%, leakage rate 2.567%, and picking efficiency 74.791 kg/h. The following combinations of experimental parameters were determined and verified: suction wind speed 25 m/s, picking roller rotational speed 31 r/min, upper cleaning baffle angle −19°, and under cleaning baffle angle 19.5°. Based on the parameters, three experiments were carried out and averaged, and the results were: impurity rate 1.537%, breakage rate 0.902%, leakage rate 2.592%, picking efficiency 73.374 kg/h. The prediction results were 3.09%, 0.78%, 0.97%, 1.89%, respectively, and the error difference is small, so the optimal parameters of the pneumatic jujube harvester are suction wind speed 25 m/s, picking roller rotational speed 31 r/min, upper cleaning baffle angle −19°, lower cleaning baffle angle 19.5°.

6. Conclusions

This paper presents a pneumatic jujube harvester. Through theoretical analysis and calculation, a self-regulating double-roller jujube picking roller was designed, supplemented by negative-pressure air flow, to pick fresh jujubes from the tree. The double-layer cleaning device was used to separate the jujubes from impurities, completing the harvesting process of fresh jujubes from the tree. The research group conducted a jujube harvesting experiment in the jujube orchard using this jujube harvester. The test results showed that when the suction wind speed was 25 m/s, the speed of the picking roller was 31 r/min, the inclination angle of the upper cleaning baffle was −19°, and the inclination angle of the lower cleaning baffle was 19.5°, the impurity rate of the jujubes was 1.537%, the damage rate was 0.902%, the missed picking rate was 2.592%, and the picking efficiency was 73.374 kg/h, achieving good mechanical harvesting of jujubes. Compared with the existing vibrating or pneumatic mechanical harvesting methods for jujubes, this jujube harvester adopts a combined mechanical and pneumatic harvesting method, achieving non-destructive and efficient harvesting of fresh jujubes from the tree.

Author Contributions: Conceptualization: H.H. and W.N.; Methodology: H.H., B.X. and W.N.; Validation: H.H., W.N., Q.W., H.Y. and R.Z.; Formal analysis: H.H., B.X. and Q.C.; Investigation: H.H. and W.N.; Resources: H.H., W.N. and Q.C.; Data curation: H.H., W.N., Q.W., H.Y., J.Z. and R.Z.; Writing—original draft: H.H. and W.N.; Writing—review and editing: H.H., W.N., Q.W., H.Y., J.Z. and R.Z.; Supervision: H.H., B.X. and Q.C.; Project administration: H.H. and Q.C.; Funding acquisition: H.H. and Q.C. All authors have read and agreed to the published version of the manuscript.

Funding: This study was supported by the Science and Technology Innovation Fund of Shanxi Agricultural University (2020BQ48); The project of Central Guided Local Science and Technology Development Fund (YDZJSX20231C008); the project of Shanxi Provincial Science and Technology Major Special Program of 2022 "Unveiling the List of Commander-in-Chief" (NJ23-07-193); the scientific research project of Shanxi Provincial Outstanding Doctoral Work Reward Fund in Jin (SXYBKY2019050); Youth Science and Technology Innovation Fund of Shanxi Agricultural University (2018015).

Data Availability Statement: No new data were created or analyzed in this study.

Conflicts of Interest: The authors declare no conflict of interest.

References

1. Edo, G.I.; Nwachukwu, S.C.; Makia, R.S.; Jikah, A. Unveiling the Chinese or jujube (*Ziziphus jujuba*); its phytochemical, botanical, industrial and pharmacological properties: A review. *Phytochem. Rev.* **2024**, 1–34. [CrossRef]
2. Yuan, Y.; Bai, S.; Niu, K.; Zhou, L.; Zhao, B.; Wei, L.; Xiong, S.; Liu, L. Research progress of mechanized harvesting technology and equipment for forest fruits. *J. Agric. Eng.* **2022**, *38*, 53–63.
3. Ferreira, M.D.; Sanchez, A.C.; Braunbeck, O.A.; Santos, E.A. Harvesting fruits using a mobile platform: A case study applied to citrus. *Eng. Agric.* **2018**, *38*, 293–299. [CrossRef]
4. Afsah-Hejri, L.; Homayouni, T.; Toudeshki, A.; Ehsani, R.; Ferguson, L.; Castro-García, S. Mechanical harvesting of selected temperate and tropical fruit and nut trees. *Hortic. Rev.* **2022**, *49*, 171–242.
5. Zhang, Z.; Heinemann, P.H.; Liu, J.; Baugher, T.A. The development of mechanical apple harvesting technology: A review. *Trans. ASABE* **2016**, *59*, 1165–1180. [CrossRef]
6. Bu, L.; Chen, C.; Hu, G.; Zhou, J.; Sugirbay, A.; Chen, J. Investigating the dynamic behavior of an apple branch-stem-fruit model using experimental and simulation analysis. *Comput. Electron. Agric.* **2021**, *186*, 106–224. [CrossRef]
7. Li, P.; Lee, S.; Hsu, H.Y. Review on fruit harvesting method for potential use of automatic fruit harvesting systems. *Procedia Eng.* **2011**, *23*, 351–366. [CrossRef]
8. Zhuo, P.; Li, Y.; Wang, B.; Jiao, H.; Wang, P.; Li, C.; Niu, Q.; Wang, L. Analysis and experimental study on vibration response characteristics of mechanical harvesting of jujube. *Comput. Electron. Agric.* **2022**, *203*, 107446. [CrossRef]
9. He, H.; Zhang, W.; Chen, D.; Jin, Z. The Kinematic Modeling and Simulation of Rotating-Contact Jujube Harvest Method. In Proceedings of the 2016 5th International Conference on Measurement, Instrumentation and Automation (ICMIA 2016), Shenzhen, China, 17–18 September 2016; Atlantis Press: Dordrecht, The Netherlands, 2016; pp. 214–221.
10. Hu, Y.; Feng, J.; Qiao, Y.; Yu, C.; Luo, W.; Zhang, K.; Liu, R.; Han, R. Research and validation of vibratory harvesting device for red jujube based on ADAMS and ANSYS. *Agriculture* **2023**, *13*, 1334. [CrossRef]
11. Peng, J.; Xie, H.; Feng, Y.; Fu, L.; Sun, S.; Cui, Y. Simulation study of vibratory harvesting of Chinese winter jujube (*Zizyphus jujuba* Mill. cv. Dongzao). *Comput. Electron. Agric.* **2017**, *143*, 57–65. [CrossRef]
12. Zhang, F.; Yu, F.; Li, Z.; Zhang, H.; Lan, H.P.; Li, P.; Zhang, C.J. Design and test of air-absorbing floor-standing jujube picker. *J. Fruit Tree* **2020**, *37*, 278–285. [CrossRef]
13. Zhang, X.; Bai, S.; Jin, W.; Yuan, P.; Yu, M.; Zhang, Z. Development of pneumatic short dense cultivation jujube picker. *J. Agric. Eng.* **2019**, *35*, 1–9.
14. Zhang, F.; Shao, W.; Zhu, J.; Zhang, T.; Zhao, S.; Li, P. Design and experiment of a self-propelled jujube collection strip pick-up machine. *INMATEH-Agric. Eng.* **2023**, *70*, 251–264. [CrossRef]
15. Gielis, J. A generic geometric transformation that unifies a wide range of natural and abstract shapes. *Am. J. Bot.* **2003**, *90*, 333–338. [CrossRef] [PubMed]

Disclaimer/Publisher's Note: The statements, opinions and data contained in all publications are solely those of the individual author(s) and contributor(s) and not of MDPI and/or the editor(s). MDPI and/or the editor(s) disclaim responsibility for any injury to people or property resulting from any ideas, methods, instructions or products referred to in the content.